Supporting information for

Poly(3-decylthiophene) Radical Anions and Cations in Solution: Single and

Multiple Polarons and Their Delocalization Lengths in Conjugated Polymers

Norihiko Takeda and John R. Miller[*]

Chemistry Department, Brookhaven National Laboratory, Upton, New York 11973-5000

Gel Permeation Chromatography (GPC) of P3DT

Commercially obtained poly(3-decylthiophene), P3DT was dissolved in THF and filtered through 0.45µm PTFE membrane filter. GPC was measured as previously reported.[S1]   Calibration was done with polystyrene standards.   An example of GPC trace is shown in figure S1.
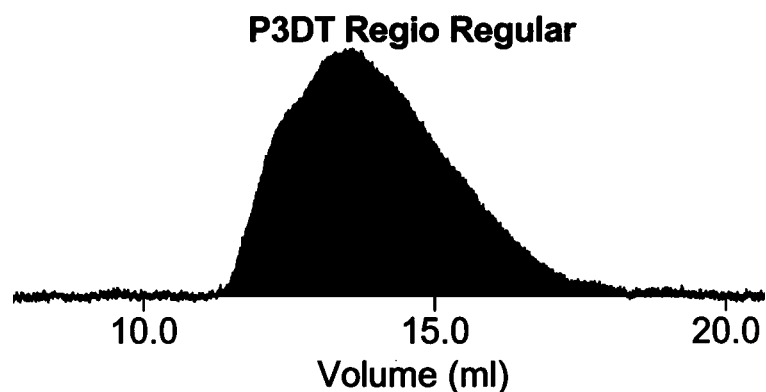

Figure S1.   A GPC trace of regioregular P3DT dissolved in THF.   The flow rate was 1 mL min^{-1}.

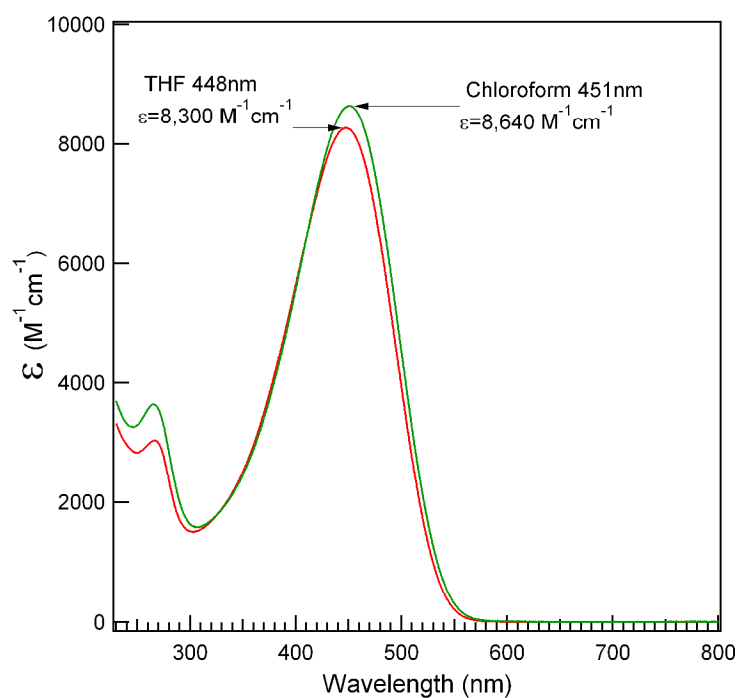**Optical absorption spectra of polythiophene and oligothiophens (nTs)**

Figure S2. Optical absorption spectra of regioregular poly(3-decylthiophene) in THF and CHCl$_3$. Extinction coefficients, ε, are per repeat unit.
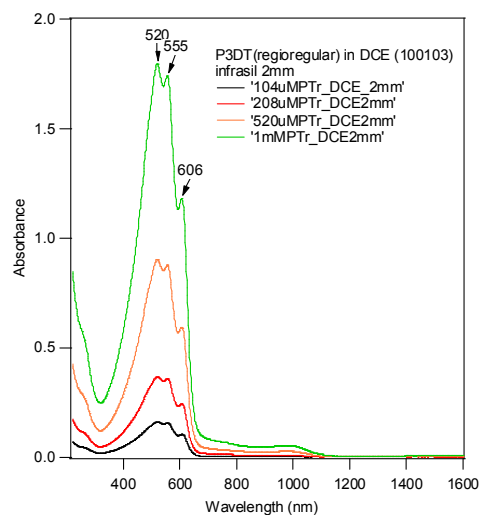

Figure S3. Optical absorption spectra of regioregular poly(3-decylthiophene) in 1,2 –dichloroethane (DCE) is red-shifted and shows structure, not seen in "good" solvents THF and chloroform. The structure indicates aggregation.[S2]
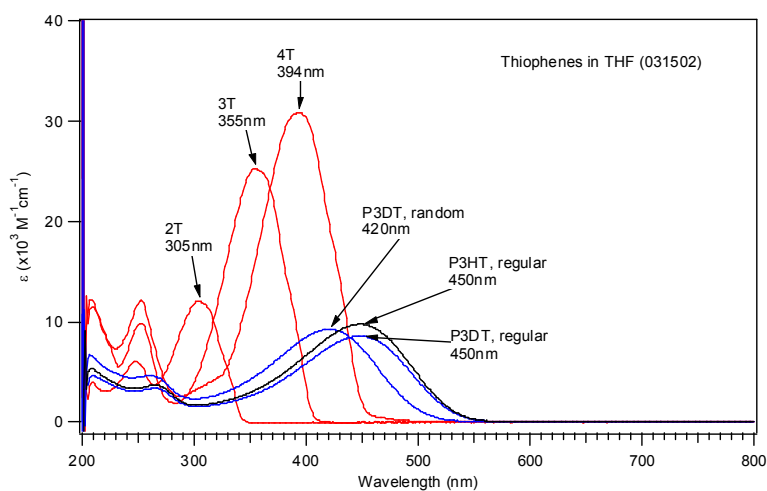
Figure S4. Optical absorption spectra in THF for oligothiophenes compared to those regioregular and regiorandom poly(3-decylthiophene) and poly(3-hexylthiophene). Extinction coefficients, ε, are per repeat unit for the polymers and per molecule for the oligomers.

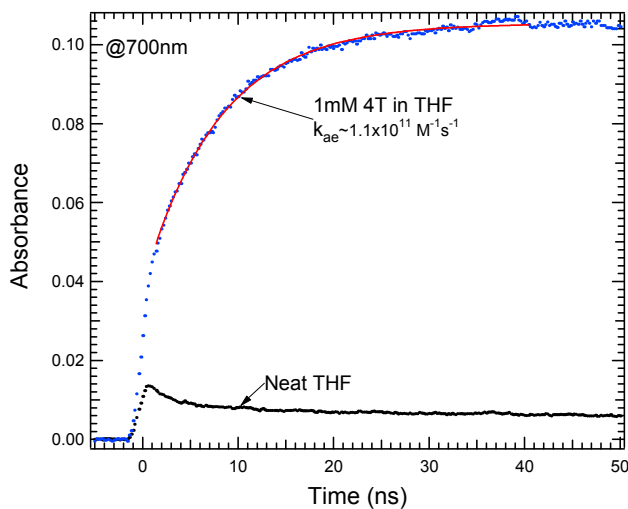**Pulse-radiolysis of quaterthiophene in THF**

Figure S5. Transient absorption of T_4 radical anion at its 700 nm maximum in THF compared to that of neat THF.
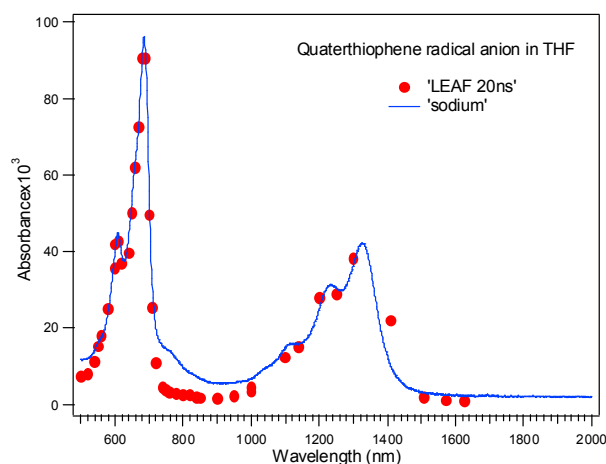
Figure S6. Transient absorption spectrum of T_4 radical anion in THF compared to the spectrum obtained by reduction of T_4 by sodium in THF.
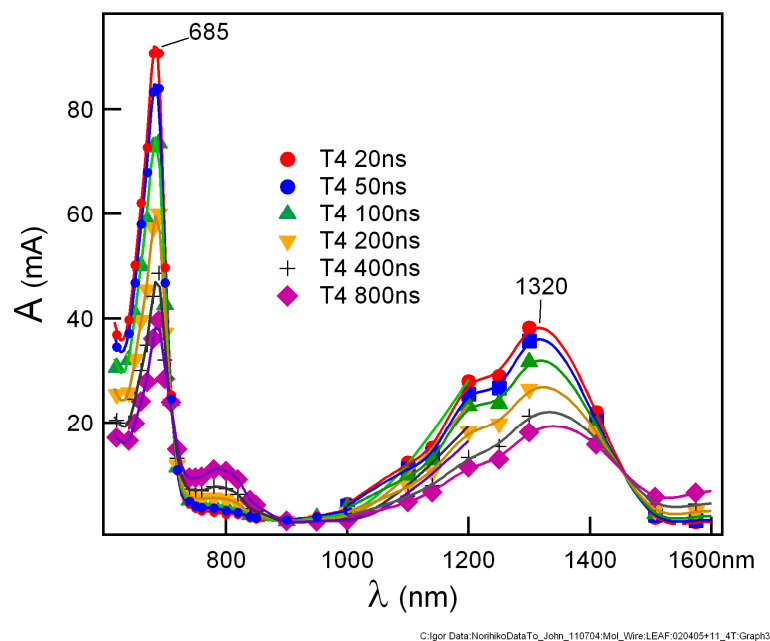

Figure S7. Transient absorption spectra of T_4 radical anion in a 1 mM solution of as-received quaterthiophene in THF. Principal absorption bands are at 685 and 1320 nm. At long times these band decay and new bands appear, particularly at ~800 nm. While this could be due to an impurity, but the pseudo first order growth of 2.5×10^5 s^{-1} at 800 nm would imply an impurity concentration of ~1 $\times 10^{-5}$ M assuming a diffusion-controlled rate constant of ~ 2.5×10^{10} M^{-1}s^{-1}. This inferred impurity concentration is 1%, too large given the 800 nm band was seen (data not shown) even after the rigorous purification (recrystallization + sublimation). Alternative explanations include formation of a dimer ($T_4^{-\bullet} + T_4 \rightleftharpoons (T_4)_2^{-\bullet}$), but Na-doping experiments support the impurity hypothesis.

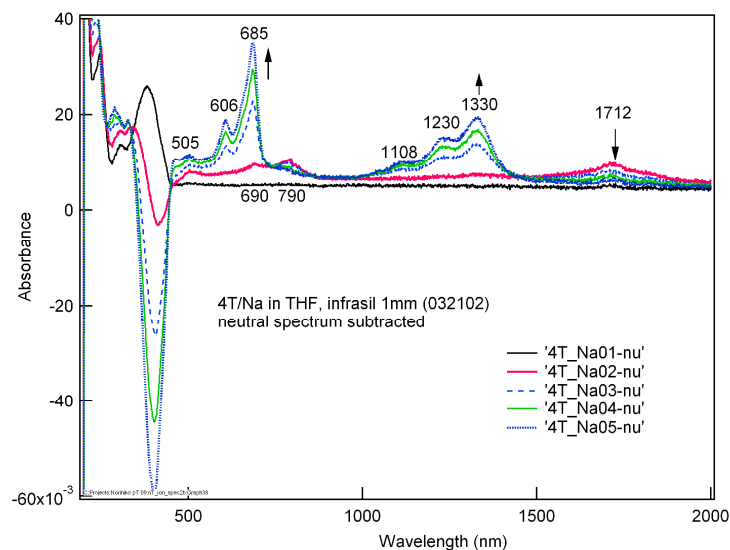# Reduction of quaterthiophene (T$_4$) by Sodium

Figure S8. Optical absorption spectra during reduction of T$_4$ by successive contact with Na metal in THF in vacuum. The spectrum of the neutral is subtracted from the spectrum for each successive exposure to Na to produce the difference spectra shown. Radical anions, T$_4^{-\bullet}$, give principal absorption bands at 685 and 1330 nm. Curiously the first exposure appears to slightly increase absorption at the neutral band (400 nm), but produces no anions. The second exposure gives another species with a spectrum different from that of T$_4^{-\bullet}$.
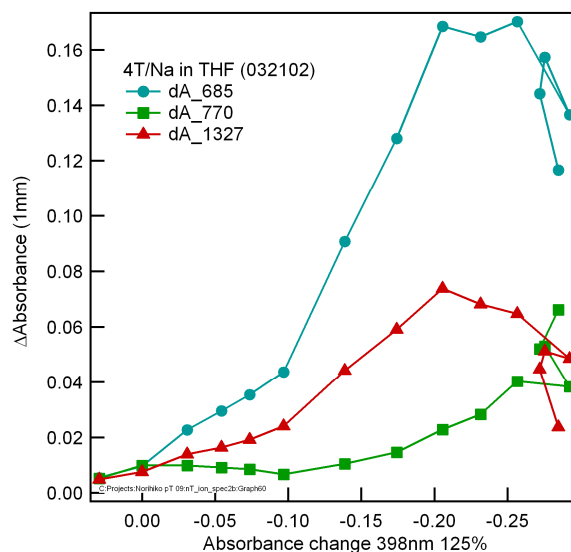

Figure S9. Absorbance changes at three wavelengths during reduction of T$_4$ by successive contact with Na metal plotted vs. the absorbance change at the 398 nm band of T$_4$ neutral. The 685 and 1327 bands due to T$_4^{-\bullet}$ reach maxima and then decrease. The band at 770 nm, assigned to T$_4^{-2}$ begins to grow near, but just before that maximum, indicating some conproportionaion (T$_4^{-\bullet}$ + T$_4^{-\bullet}$ ⇌ T$_4$ + T$_4^{-2}$) occurs.

Estimation of number of bleached neutral thiophene unit from transient absorption spectrum of P3DT anion

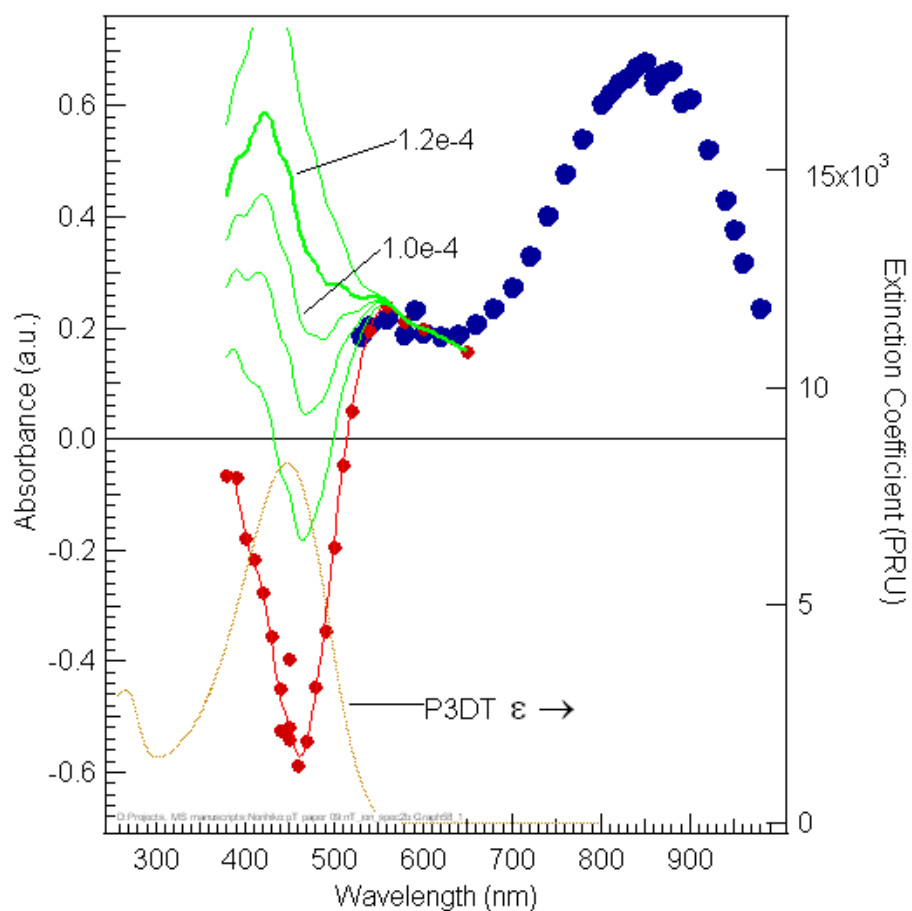*Figure S10.* Transient absorption of P3DT anions and the corresponding bleaching of the P3DT neutral band. Because the anions also absorbed in the region of P3DT neutral, different amounts of the neutral band were added to the transient spectrum to produce trial spectra (green). The actual spectrum of the anion is plausibly between the spectra for which 1.0e-4 and 1.2e-4 of the P3DT neutral spectrum were added.
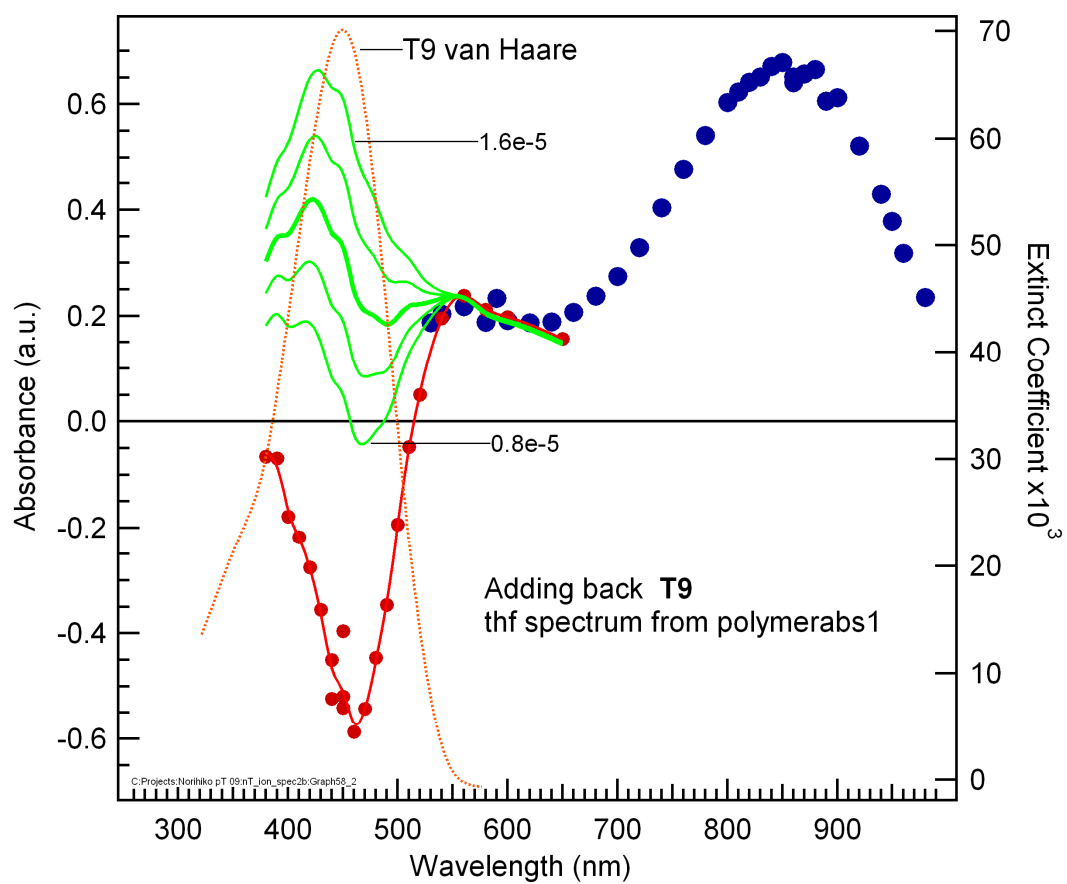
Figure S11. Like Figure S10, but adding back the spectrum of T9 oligomer by van Haare.[S3]
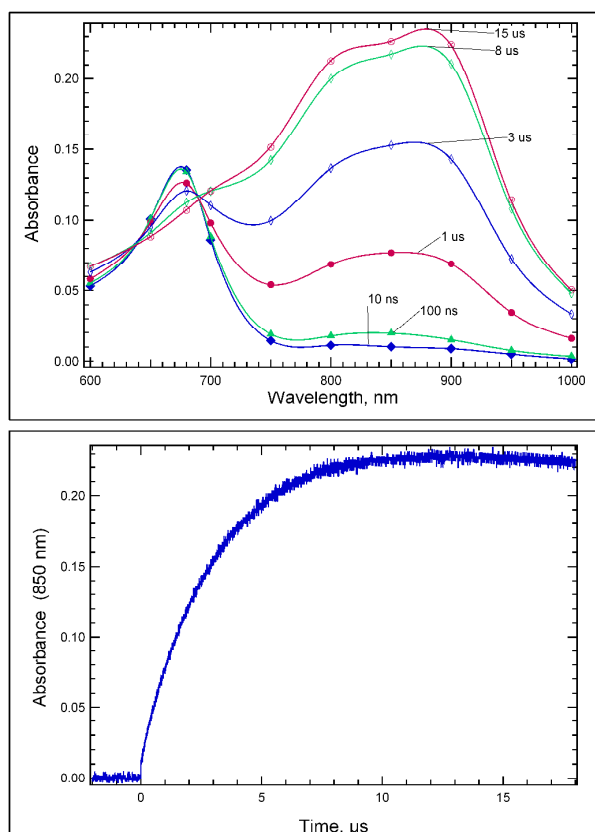
Pulse-radiolysis of P3DT in chloroform

Figure S12. Transient absorption spectra of 2.9 mM (repeat unit) P3DT + 21 mM TTA in chloroform (upper panel). The optical pathlength was 2 cm. The spectrum at 10 ns is almost exclusively due to TTA cation, but P3DT cation grows with time demonstrating transfer of a positive charge from TTA$^{\bullet+}$ to P3DT. The transient absorbance at 850 nm (lower panel) grows with a pseudo first order rate constant 3.7×10^5 s^{-1} giving a bimolecular hole transfer rate constant of 2.1×10^{10} M^{-1}s^{-1}. At 15 μs not all TTA$^{\bullet+}$ is gone; some remains in equilibrium with P3DT$^{\bullet+}$. The remaining amount is imprecise because the spectrum of P3DT$^{\bullet+}$ has shifted, probably due to ion-pairing, but it can be estimated that $33\pm15\%$ of the ions are TTA$^{\bullet+}$. For the reaction TTA$^{\bullet+}$ + P3DT $\rightleftharpoons$ TTA + P3DT$^{\bullet+}$, $K_{eq}=2600$ with an uncertainty of a factor of 2. Accordingly the potential difference E^0(P3DT$^{+/0}$) − E^0(TTA$^{+/0}$) = RT/nF lnK_{eq} is estimated to be 0.20 V at room temperature. Furthermore, the absorption coefficient of P3DT$^{\bullet+}$ at 850nm can be deduced using the initial yield of TTA$^{\bullet+}$ and the ratio of P3DT$^{\bullet+}$ produced at equilibrium estimated above. The radiolysis in chloroform created excited states of P3DT as in the case of THF solution. A contribution of triplet absorbance, found by addition of to air to remove triplets, was subtracted from the measured absorbance to calculate the absorption coefficient of P3DT$^{\bullet+}$.
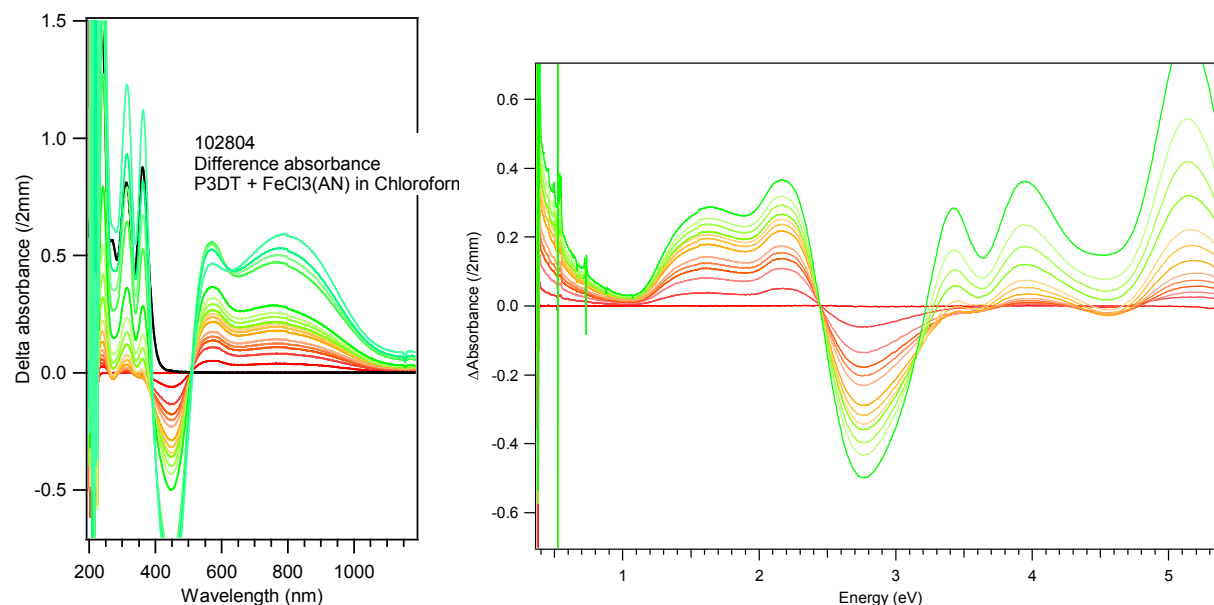
Chemical oxidation of P3DT by FeCl₃

Figure S13. Chemical oxidation by addition of FeCl₃ to P3DT in chloroform in a 2 mm cell. Aliquots of anhydrous FeCl₃ solution in acetonitrile (15 mM) were added to 1 mM (monomer) P3DT solution in chloroform. Added FeCl₃ concentration started from 15 μM and finally went to 5.3mM.

Molecular orbital calculations

Semiempirical AM1 and density functional calculations were performed using a Gaussian 03 program (Rev B04).[S4]   Geometries of series of non-alkylated oligothiophenes with n thiophene units (nTs) were optimized.   Neutral nTs were fully optimized using spin-restricted methods while planar and all-trans geometreis of mono-ions of nTs were optimized using spin-unrestricted methods. Usually AM1 optimized geometries were used as starting geometries for DFT calculations.   The B3LYP functional with 3-21G* basis set was used for most of the cases.   ROHF method and other functionals for DFT method were used for one case (8T) as a comparison.   Frequency calculations followed the each geometry optimizations which confirmed the achievement of minima.

Formation of a polaron is accompanied by geometrical changes.   Several different methods have been applied to geometry optimization of positively charged oligothiophene with n thiophene units

(*n*Ts).   Delocalization length of positive polarons and bipolarons were discussed in terms of C-C bond length alternation as well as Mulliken charge and spin density distributions.   Ranges of delocalization lengths for nT positive polaron (2 to ∞) have been reported depending on the computational methods used.[S5-S9]

In the present study series of non-alkylated oligothiophenes nT were studied by AM1 and DFT methods and different pictures for negative polarons emerged.

In the neutral form, both methods showed aromatic character of C-C length patterns although exact magnitudes of bond length alternations were different. Examples are shown for 12T in Figure S14. With AM1, dihedral angles between neighboring thiophene rings are slightly off from the coplanar angles.   With DFT, they were more coplanar but slightly bent toward the chain ends.

When one electron is attached, geometries were changed (figure S14). Geometries were constrained to be all planar and trans form as has been done for cations.[S5-S9]   AM1 predicts dramatic geometrical changes with quinoid-like bond alternation except for the ends while DFT showed smaller geometrical changes. In DFT optimized geometries, aromatic characters were still retained although some bond shortening occurs between the rings, which were more significant around the center of the chain.
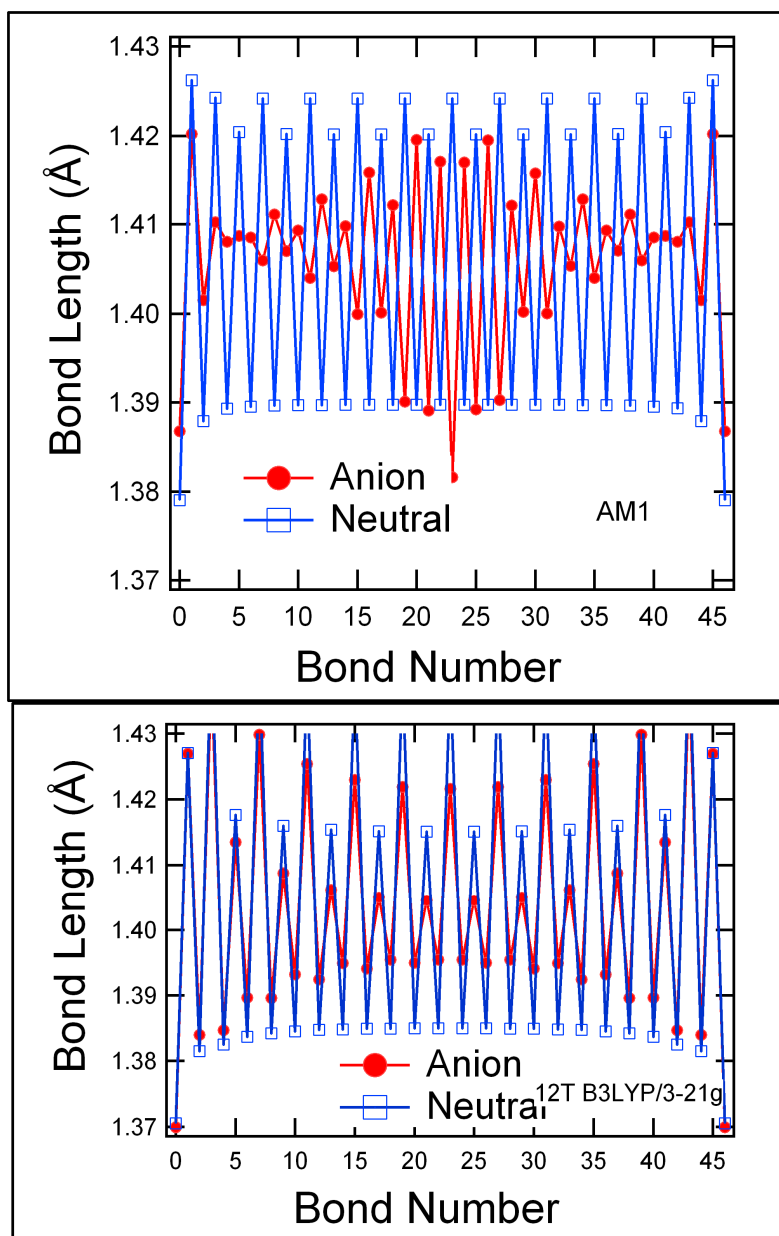
Figure S14. C-C bonds distances, R(C-C) in Ǻ for 12T computed by AM1 (top) and b3lyp/3-21g (bottom) for the neutral and radical anion. The lengths are given as a function of bond number from left to right; C-S bonds were omitted.

Mulliken charge and spin density distribution

Figure S15 shows negative charge is delocalized over 4-5 thiophene units with AM1. On the other hand, DFT with B3LYP functional does not show obvious localization at least up to 12T (figure S16). Comparison of DFT methods for 8T anion in figure S17-18 revealed different behavior of

charge distribution among different fuctional with same basis set. ROHF (had 2 imaginary frequencies) showed most localized charge and spin while BHandHLYP and BHandH showed similar localization found by Geskin et al.[S9] for nT cation. Pure DFT (BLYP) showed no localization of charge as shown for cations by Moro.[S8] Other hybrid DFT with less HF exchange (B3LYP, B1LYP, B1B95, and B3PW91) showed intermediate behavior between BLYP and bHandHLYP.
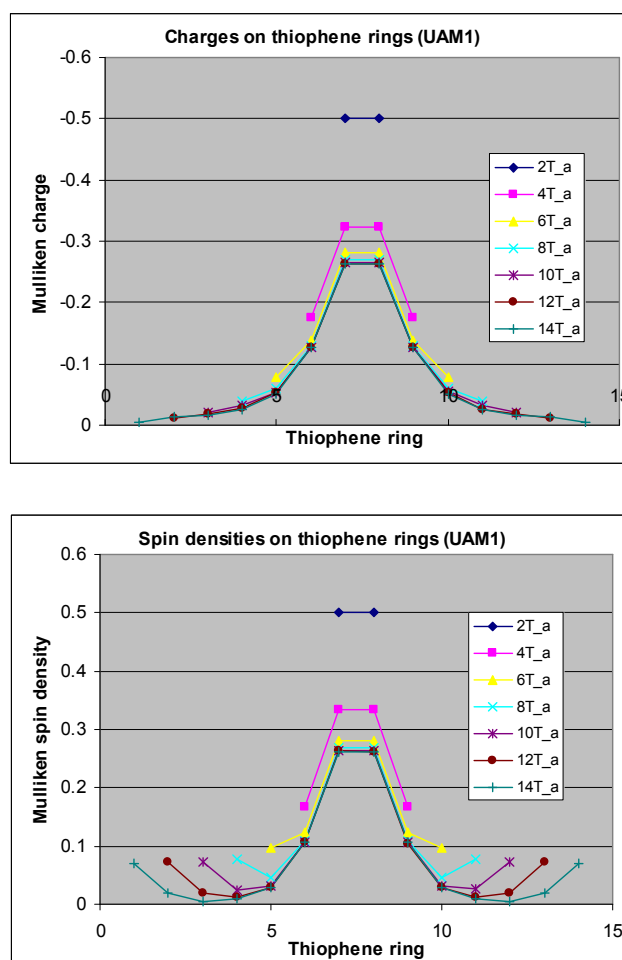

Figure S15. Mullikan charges and spin densities per thiophene ring in oligothiophene anions, $T_n^{-\bullet}$ (n=2,4,6,8,10,12, and 14) computed by the AMl calculations.
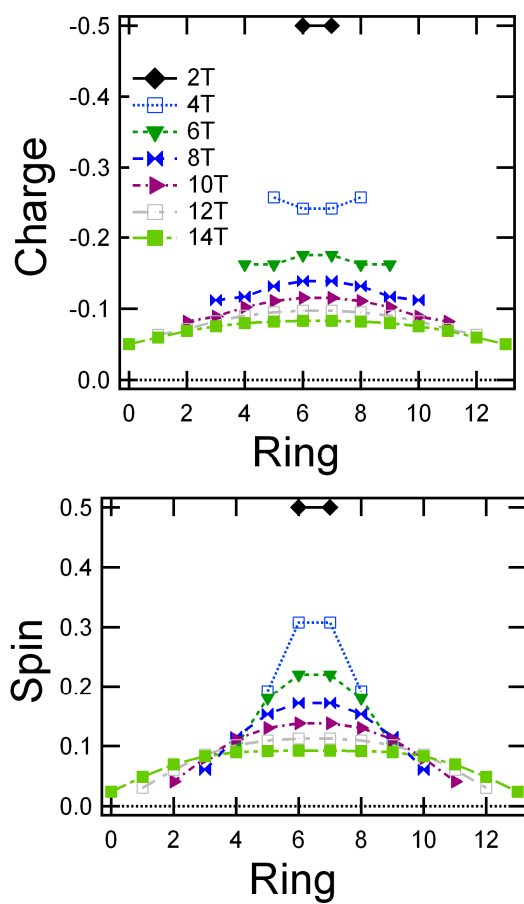
Figure S16. Mullikan charges and spin densities per thiophene ring in oligothiophene anions, $T_n^{-\bullet}$ (n=2,4,6,8,10,12, and 14) computed by the hybrid density functional calculations. DFT-based methods may overestimate delocalization.
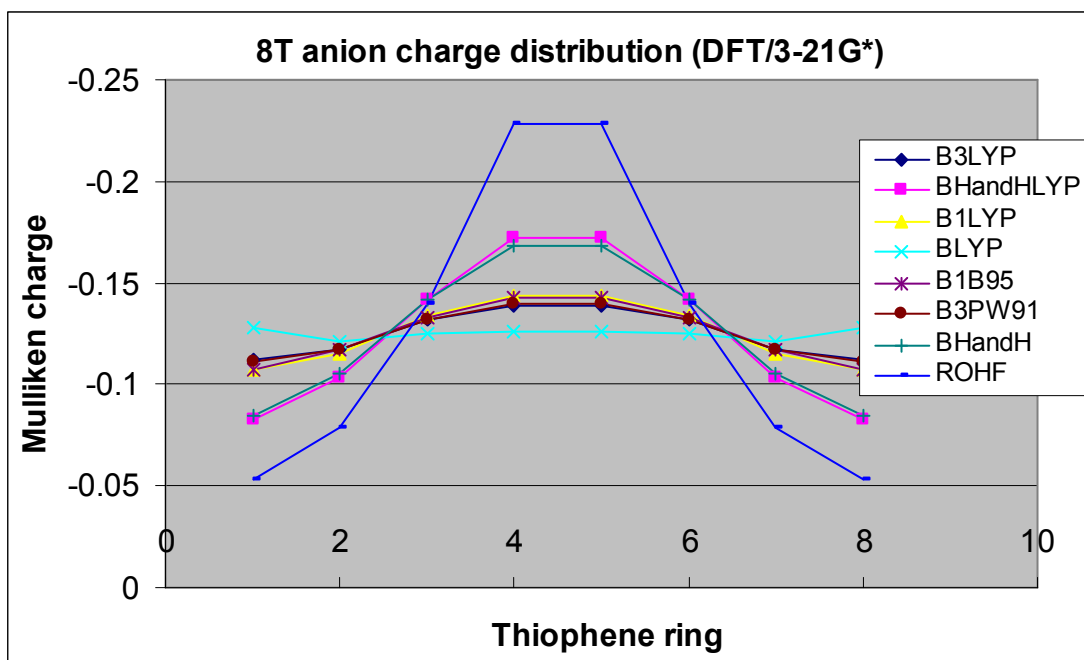
Figure S17. Charges per thiophene ring in oligothiophene anions, $T_8^{-\bullet}$ computed by the varied methods showing the progression of delocalization as less HF is included.

Figure S18. Spin density per thiophene ring in oligothiophene anions, $T_8^{-\bullet}$ computed by the varied methods showing the progression of delocalization as less HF is included.
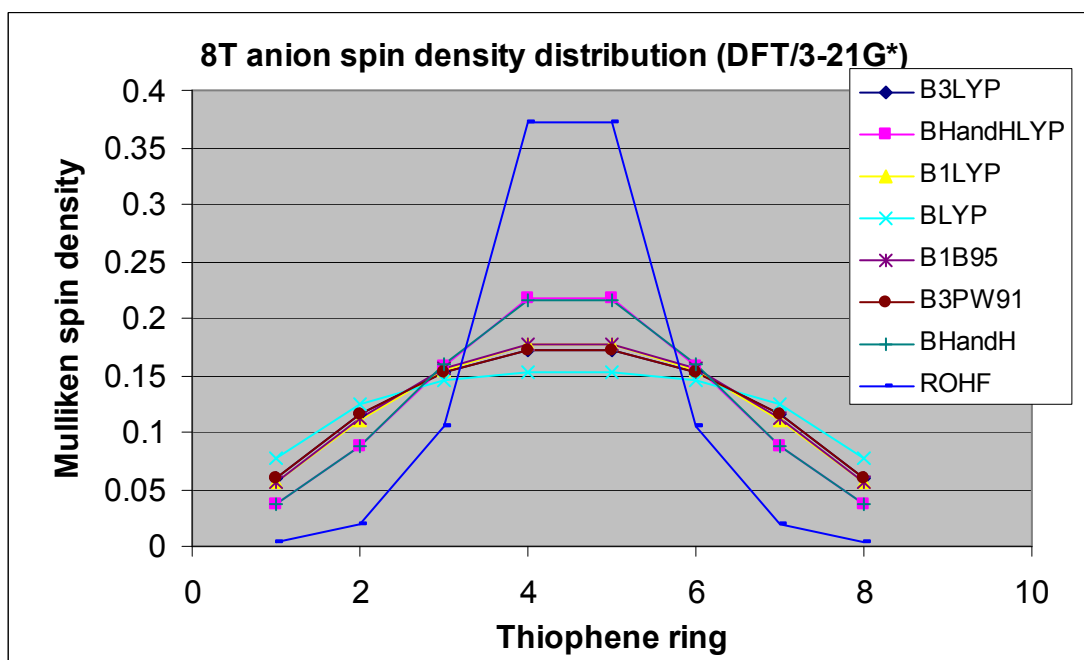
References

(S1)   Takeda, N.; Asaoka, S.; Miller, J. R. *J. Am. Chem. Soc.* **2006**, *128*, 16073-16082.

(S2)   Rumbles, G.; Samuel, I. D. W.; Magnani, L.; Murray, K. A.; DeMello, A. J.; Crystall, B.; Moratti, S. C.; Stone, B. M.; Holmes, A. B.; Friend, R. H. *Synth. Met.* **1996**, *76*, 47-51.

(S3)   van Haare, J.; Havinga, E. E.; van Dongen, J. L. J.; Janssen, R. A. J.; Cornil, J.; Bredas, J. L. *Chem. Eur. J.* **1998**, *4*, 1509-1522.

(S4)   Gaussian 03, Revision B.04, Frisch, M. J.; Trucks, G. W.; Schlegel, H. B.; Scuseria, G. E.; Robb, M. A.; Cheeseman, J. R.; Montgomery, Jr., J. A.; Vreven, T.; Kudin, K. N.; Burant, J. C.; Millam, J. M.; Iyengar, S. S.; Tomasi, J.; Barone, V.; Mennucci, B.; Cossi, M.; Scalmani, G.; Rega, N.; Petersson, G. A.; Nakatsuji, H.; Hada, M.; Ehara, M.; Toyota, K.; Fukuda, R.; Hasegawa, J.; Ishida, M.; Nakajima, T.; Honda, Y.; Kitao, O.; Nakai, H.; Klene, M.; Li, X.; Knox, J. E.; Hratchian, H. P.; Cross, J. B.; Bakken, V.; Adamo, C.; Jaramillo, J.; Gomperts, R.; Stratmann, R. E.; Yazyev, O.; Austin, A. J.; Cammi, R.; Pomelli, C.; Ochterski, J. W.; Ayala, P. Y.; Morokuma, K.; Voth, G. A.; Salvador, P.; Dannenberg, J. J.; Zakrzewski, V. G.; Dapprich, S.; Daniels, A. D.; Strain, M. C.; Farkas, O.; Malick, D. K.; Rabuck, A. D.; Raghavachari, K.; Foresman, J. B.; Ortiz, J. V.; Cui, Q.; Baboul, A. G.; Clifford, S.; Cioslowski, J.; Stefanov, B. B.; Liu, G.; Liashenko, A.; Piskorz, P.; Komaromi, I.; Martin, R. L.; Fox, D. J.; Keith, T.; Al-Laham, M. A.; Peng, C. Y.; Nanayakkara, A.; Challacombe, M.; Gill, P. M. W.; Johnson, B.; Chen, W.; Wong, M. W.; Gonzalez, C.; and Pople, J. A.; Gaussian, Inc., Wallingford CT, 2004.

(S5)   Cornil, J.; Beljonne, D.; Bredas, J. L. *J. Chem. Phys.* **1995**, *103*, 842-849.

(S6)   Brocks, G. *Synth. Met.* **1999**, *102*, 914-915.

(S7)   Casado, J.; Hernandez, V.; Ramirez, F. J.; Navarrete, J. T. L. *J. Mol. Struct.: Theochem* **1999**, *463*, 211-216.

(S8)   Moro, G.; Scalmani, G.; Cosentino, U.; Pitea, D. *Synth. Met.* **2000**, *108*, 165-172.

(S9)   Geskin, V. M.; Bredas, J. L. *Int. J. Quantum Chem.* **2003**, *91*, 303-310.